

Quantum Measurement Induced Radiative Processes in Continuously Monitored Optical Environments

Eldhose Benny¹ and Sreenath K. Manikandan^{2,*}

¹*Department of Physics, National Institute of Technology Calicut, Kozhikode, Kerala 673601, India*

²*Nordita, Stockholm University and KTH Royal Institute of Technology,*

Hannes Alfvéns väg 12, SE-106 91 Stockholm, Sweden

(Dated: November 14, 2024)

We investigate the emission characteristics of a measurement-driven quantum emitter in a continuously monitored optical environment. The quantum emitter is stimulated by observing the Pauli spin along its transition dipole that maximally non-commutes with the Hamiltonian of the emitter. It also exchanges energy resonantly with the optical environment, observable as quantum jumps corresponding to the absorption or emission of a photon and the null events where the quantum emitter did not make a jump. We characterize the finite-time statistics of quantum jumps and estimate their covariance and precision using the large deviation principle. We also generalize our considerations to coarse-grained measurements of the optical field and compute the finite-time statistics of the sum of absorption and emission events, which we refer to as the negation of null events in our problem. While the statistics of absorption and emission events are generically sub-Poissonian, our analysis reveals a spin-measurement-induced transition from super-Poissonian to sub-Poissonian in their sum. Our findings suggest that quantum measurement-induced fluctuations can be a useful alternative to coherent drives for stimulating radiative transitions having controllable emission characteristics, with implications extending to atomic and nuclear clocks.

I. INTRODUCTION

Quantum emitters which can produce single photons with non-classical features on demand, as well as photodetectors which can probe and verify their non-classicality are essential elements of the quantum photonics toolkit for quantum technologies [1–5]. Observing sub-Poissonian statistics is particularly exciting in these settings, as it cannot be explained within a classical framework [6–8]. Null detection events, where the detector does not click within the measurement window, also offer an exciting problem of fundamental interest as the null detections also carry the valuable information that the quantum emitter is less likely to be in its excited state from which the emission process occurs. Hence they induce a statistically irreversible evolution towards the quantum ground state of the emitter even when no detections are registered. Null measurements are also of great significance in the context of the quantum measurement problem [9], as they belong to the class of quantum measurements that can be reversed or undone in experiments with sequential measurements, with some probability of success [10, 11].

Good emitters are also good detectors, and characterizing their spontaneous emission process, which also lacks classical reasoning, is fundamental to both quantum emitters and detectors alike [12]. Its controlled manipulations including reversibility are topics of great contemporary interest [13–19]. Spontaneous emission is caused by the quantum emitter interacting with vacuum modes of the radiation field, and can be under-

stood as driven by quantum fluctuations of the vacuum. The quantum emitter can also be coherently driven and the resulting resonant fluorescence emission can be monitored time-continuously via different detection schemes, photon counting, homodyne, or heterodyne detection of the emitted photon [15, 16, 20]. Such detection schemes are currently accessible experimentally in artificial atoms [21–23] where they also find various applications in readout and feedback control [24–26].

We consider an alternate paradigm where quantum fluctuations of a different origin drive the radiative processes of a quantum emitter. This is by stimulating the emitter using quantum measurements of the Pauli spin $\hat{\sigma}_x$ along its transition dipole, a spin direction that maximally not-commutes with the Hamiltonian of the quantum emitter (see Fig. 1). The quantum emitter effectively

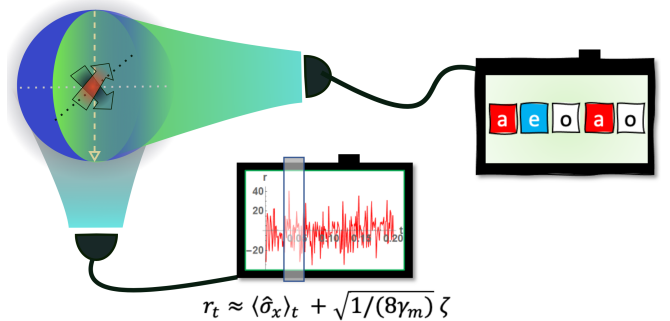


FIG. 1. A quantum emitter driven by the quantum measurements of the Pauli spin $\hat{\sigma}_x$ along its transition dipole moment. The induced radiative processes [absorption (a), emission (e), and null events(o)] are recorded by continuously monitoring the optical environment.

* sreenath.k.manikandan@su.se

acts as a transducer in our setting, converting the fluctuations caused by quantum-noise-limited measurements [9] of the Pauli spin $\hat{\sigma}_x$ to produce a series of events of varying quantum statistics.

The quantum jumps are monitored by observing the optical environment which refreshes rapidly to maintain its average population. This also marks a crucial difference to standard detection scenarios in that we consider the optical environment is generically not in its vacuum state [27]. Since measurement of the optical field can probe the dynamics of the quantum emitter, the rapidly refreshing optical environment can also be thought of as resonant photodetector in the single-mode approximation for the optical field [28]. A limiting scenario corresponds to when the photodetector is in its vacuum state. This was studied in detail by one of the authors in [29], where it was shown that the quantum measurement of the spin induces the emission of photons with sub-Poissonian statistics observable at the detector. In the generic scenarios within the rotating wave approximation that we consider in the present manuscript, initially populated photodetectors can either register clicks by absorbing or emitting a photon, or not produce a click (describing a null event) conditioned on the quantum state of the emitter. The paradigm we consider is also relevant to experiments, since resonance fluorescence in generic environments (such as in squeezed vacuum state [30]), has been investigated in experiments [31]. Note that these generic environments offers a much richer scenario without the rotating wave approximation [30, 31], which we limit ourselves to in the present work for simplicity. We derive the relevant measurement operators and show that the statistics of radiative processes can be predicted using the principle of large deviation in appropriate limits. Our work is naturally generalizable to other generic scenarios that could be of broader interest.

Large deviation theory and comparable approaches have made important contributions to our current understanding of quantum transport in nanoscale quantum devices and solid-state qubits [32–35]. Since the total number of absorption or emission events is much smaller compared to the total number of null events in the optical detection scenarios we consider, they agree with good precision to the results of the large deviation theory. Trying to compute the statistics of null events directly can be pathological as it depends on the discretization in time that seems arbitrary (although waiting time-distributions can be computed and are statistically meaningful [11]). Instead, we make statistically meaningful inferences about the null events from the joint statistics of absorption and emission events, as together they are complete. We compute the covariance of the absorption and emission events using the large deviation theory to estimate the statistics of the sum of absorption and emission events, which we refer to as the negation of null events in our problem. One of our key findings is that, while the statistics of absorption and emission events remain sub-Poissonian, the statistics of their sum (the negation

of null events) transition from super-Poissonian to sub-Poissonian, by increasing the rate at which the quantum emitter’s Pauli spin $\hat{\sigma}_x$ along its transition dipole is measured. This demonstrates that the covariance of observing the quantum jumps also contains additional extractable information about the quantum nature of the underlying dynamics, not already evident from the statistics of absorption or emission events monitored individually. Physically they can be associated with the distribution of null detection events within a finite-time window of monitoring the quantum jumps. While it is only a specific quantum emission scenario we consider, it reinforces our understanding that the null detection events in quantum mechanics are not non-informative. The negation of their finite-time statistics we estimate can also be relevant in other comparable scenarios, for example, in the avenue of quantum sensing of weak forces where the null events are not rare [36].

Inducing radiative processes by the transduction of quantum measurement fluctuations may also be relevant for atomic clocks [37], where it may have the potential to excite transitions that are difficult to induce using traditional alternatives. There have been important recent progresses in exciting nuclear optical transitions using coherent drives in the context of atomic clocks, which also shed light on the difficulty in generating controlled emission scenarios involving nuclear transitions [38, 39]. Quantum measurement engineering of the type we consider can be an interesting alternative to consider in such settings, as it offers a fundamentally different mechanism for driving radiative transitions. There have been some early suggestions on the role of the quantum Zeno effect in nuclear transitions [40] to which the generalized emission scenarios we consider are certainly relatable. Our proposals are certainly accessible in artificial atom-clock scenarios [29, 41–43], where they can be used as analog systems to further explore the impact of quantum measurement engineering in real atomic and nuclear transitions.

II. THE DYNAMICS

We consider a continuously monitored quantum emitter interacting with a photodetector that is initially populated. A limiting, yet comparable scenario assuming the photodetector in vacuum was considered in Ref. [29], where the finite-time statistics of emission and null events were computed. The key novelty here is that we consider an initially populated photodetector that can keep track of the quantum emitter’s complete radiative processes: emission, absorption, and null events. The two-level quantum emitter has energies 0 and Ω , with the free Hamiltonian of the quantum emitter given by $\hat{H}_0 = \Omega|e\rangle\langle e|$. For electronic or generic charge (q) transitions between the ground state $|g\rangle \equiv |\psi_g\rangle$ and the excited state $|e\rangle \equiv |\psi_e\rangle$, we can define a transition dipole operator (that couples to external electric fields or coherent

drives) as,

$$\hat{\mathbf{d}} = q\langle\psi_e|\hat{\mathbf{r}}|\psi_g\rangle|\psi_e\rangle\langle\psi_g| + q\langle\psi_g|\hat{\mathbf{r}}|\psi_e\rangle|\psi_g\rangle\langle\psi_e|. \quad (1)$$

For real electronic or charge wavefunctions $\psi_{e(g)}(\mathbf{r})$, $\langle\psi_e|\hat{\mathbf{r}}|\psi_g\rangle = \langle\psi_g|\hat{\mathbf{r}}|\psi_e\rangle$ we can write,

$$\hat{\mathbf{d}} = d\hat{\sigma}_x, \quad \text{where } d = q\langle\psi_g|\hat{\mathbf{r}}|\psi_e\rangle \in R, \quad (2)$$

and $\hat{\sigma}_x = |e\rangle\langle g| + |g\rangle\langle e|$ is the Pauli spin observable along the x direction. Instead of applying a coherent drive to stimulate the emitter, we now consider stimulating the quantum emitter's radiative processes by continuously observing its transition dipole operator, which does not commute with the Hamiltonian of the quantum emitter. Since the transition dipole operator is proportional to $\hat{\sigma}_x$, observing the quantum emitter's Pauli spin $\hat{\sigma}_x$ is equivalent to monitoring the transition dipole itself. We can use the following spin measurement operators [44],

$$\hat{M}(r_t) = (4\epsilon_m)^{1/4} \exp[-2\epsilon_m(r_t\hat{\mathbb{I}} - \hat{\sigma}_x)^2]/\pi^{1/4}, \quad (3)$$

where $\epsilon_m = \gamma_m dt$, γ_m is the continuous spin measurement rate, and dt is the time-interval between two successive measurements. The time-continuous readout signal r_t at any given time can be represented as $r_t = \langle\sigma_x\rangle_t + \sqrt{1/(8\gamma_m)}\zeta$, where ζ is a delta-correlated white noise process with variance $1/dt$. The mapping to transition dipole also suggests a natural way to implement the Pauli spin $\hat{\sigma}_x$ measurement by engineering quantum measurement interactions to the transition dipole of the quantum emitter (or to the position $\hat{\mathbf{r}}$ of the electron or charged particle in the unharmonic potential), however, note that Pauli spin measurements can be implemented in practice in different ways which are all mathematically equivalent. We also leverage this flexibility, as will be shown briefly, we do not need to keep track of the measurement outcomes in order to stimulate the quantum emitter. It is sufficient to engineer spin dephasing along the transition dipole, corresponding to unconditional spin measurement dynamics of the Pauli spin $\hat{\sigma}_x$.

We now proceed to the details of observing the radiative processes of the quantum emitter. Starting from the interaction Hamiltonian,

$$\hat{H}_{int}dt = \sqrt{\gamma_w dt}(\hat{\sigma}_+\hat{a} + \hat{\sigma}_-\hat{a}^\dagger), \quad (4)$$

we obtain the following measurement operators to leading order corresponding to the radiative events (see the appendix),

$$\hat{M}_w(e) \approx -i \begin{pmatrix} 0 & 0 \\ \sqrt{\langle n \rangle + 1}\epsilon_w & 0 \end{pmatrix}, \quad (5)$$

$$\hat{M}_w(a) \approx -i \begin{pmatrix} 0 & \sqrt{\langle n \rangle}\epsilon_w \\ 0 & 0 \end{pmatrix}, \quad (6)$$

$$\hat{M}_w(o) \approx \begin{pmatrix} \sqrt{1 - \langle n \rangle + 1}\epsilon_w & 0 \\ 0 & \sqrt{1 - \langle n \rangle}\epsilon_w \end{pmatrix}, \quad (7)$$

where $\epsilon_w = \gamma_w dt$, γ_w is the spontaneous emission rate and $\langle n \rangle$ is the population of the excited photodetector. The labels a, e, o correspond to the absorption, emission, and null events respectively. The conditional time evolution of the quantum emitter for an infinitesimal time interval dt is given by,

$$\rho(t+dt) = \frac{\hat{\mathcal{M}}_{dt}(r_t, k)\rho(t)\hat{\mathcal{M}}_{dt}^\dagger(r_t, k)}{\text{tr}\{\hat{\mathcal{M}}_{dt}(r_t, k)\rho(t)\hat{\mathcal{M}}_{dt}^\dagger(r_t, k)\}}, \quad (8)$$

where $\hat{\mathcal{M}}_{dt}(r_t, k) = e^{-i\hat{H}_0 dt}\hat{M}_w(k)\hat{M}(r_t)$, where $-\infty < r_t < \infty$ is the continuous spin readout, and $k \in \{a, e, o\}$ represent the observed radiative process. Note that the quantum state of the emitter evolves even for the null result. Going forward, since we are only interested in the statistics of observable radiative processes, we will limit (including in our simulations) to semi-conditional dynamics that average over different realizations of the spin measurement outcomes r_t . This will have an effect similar to adding a dephasing noise, along the $\hat{\sigma}_x$ direction.

The unconditional dynamics is obtained by averaging over the measurement outcomes of both the spin and radiative processes,

$$\rho(t+dt) = \sum_k \int dr \hat{\mathcal{M}}_{dt}(r_t, k)\rho(t)\hat{\mathcal{M}}_{dt}^\dagger(r_t, k). \quad (9)$$

To small dt , one obtains the unconditional master equation of the following form (note that ρ now represents the unconditional density matrix, however, we use the same symbol for simplicity),

$$\begin{aligned} \frac{d\rho}{dt} &= -i[\hat{H}_0, \rho] - \gamma_m[\hat{\sigma}_x, [\hat{\sigma}_x, \rho]] \\ &+ \gamma_w(\langle n \rangle + 1)[\hat{\sigma}_-\rho\hat{\sigma}_+ - (\hat{\sigma}_+\hat{\sigma}_-\rho + \rho\hat{\sigma}_+\hat{\sigma}_-)/2] \\ &+ \gamma_w\langle n \rangle[\hat{\sigma}_+\rho\hat{\sigma}_- - (\hat{\sigma}_-\hat{\sigma}_+\rho + \rho\hat{\sigma}_-\hat{\sigma}_+)/2]. \end{aligned} \quad (10)$$

The steady state of the unconditional dynamics is given by $\rho_s = \text{diag}\{p, 1-p\}$, where

$$p = \frac{2\gamma_m + \gamma_w\langle n \rangle}{4\gamma_m + \gamma_w(2\langle n \rangle + 1)}. \quad (11)$$

The only assumption made in arriving at the above form is that the photodetector, or the optical field is rapidly refreshing to a quantum state of the same average occupation, $\langle n \rangle$. The Gorini-Kossakowski-Sudarshan-Lindblad form of the master equation indeed suggests that the result should hold for a thermal state of the environment with $\langle n \rangle \rightarrow \bar{n}$, the average thermal population of the environment. This is indeed true, and in fact, assuming rapid resetting of the optical environment, the conclusion can be extended to any arbitrary state of the environment with $\langle n \rangle$ being the average population of the environment, provided we make the rotating wave approximation for the interaction between the quantum emitter and its environment (see the appendix). In what follows, we will

assume this generality, however, note that generalizing our considerations beyond the rotating wave approximation is certainly interesting, as it can probe interesting quantum correlations in the environment [31].

To compute the observable statistics numerically, we simulate the conditional dynamics of the quantum emitter. However, their statistics can be approximated analytically in closed form using the principle of large deviation. This technique has been applied to compute the statistics of resonance fluorescence (with the photodetector in the vacuum state) from coherently driven atoms [45], and measurement-driven artificial atoms [29]. In our generalized setting, we obtain the relevant moment-generating function $\theta(s_a, s_e)$ as the largest real eigenvalue of the following tilted Lindblad generator,

$$\begin{aligned} W(s_a, s_e)[\rho] = & -i[\hat{H}_0, \rho] - \gamma_m[\hat{\sigma}_x, [\hat{\sigma}_x, \rho]] \\ & + \gamma_w(\langle n \rangle + 1)(e^{-s_e}\hat{\sigma}_-\rho\hat{\sigma}_+ - \frac{1}{2}\{\hat{\sigma}_+\hat{\sigma}_-\rho\}) \\ & + \gamma_w\langle n \rangle(e^{-s_a}\hat{\sigma}_+\rho\hat{\sigma}_- - \frac{1}{2}\{\hat{\sigma}_-\hat{\sigma}_+\rho\}), \end{aligned} \quad (12)$$

where the s_a and s_e are the tilt parameters. We obtain the following result for the moment generating function,

$$\theta(s_a, s_e) = \frac{1}{2}[-(4\gamma_m + \gamma_w + 2\gamma_w\langle n \rangle) + e^{-(s_a+s_e)}\sqrt{g}], \quad (13)$$

where,

$$\begin{aligned} g = & e^{s_a+s_e}\{4\gamma_w(\langle n \rangle + 1)(2e^{s_a}\gamma_m + \gamma_w\langle n \rangle) \\ & + e^{s_e}[e^{s_a}(16\gamma_m^2 + \gamma_w^2) + 8\gamma_m\gamma_w\langle n \rangle]\} \end{aligned} \quad (14)$$

Compared to Ref. [29] which is recovered in the limit $\langle n \rangle \rightarrow 0$, the moment generating function given above is more general, allowing to predict the statistics of the absorption, emission events, and their covariances as shown below.

III. RESULTS

The moments of observed radiative events can be estimated from the large-deviation-approximate form of the moment-generating function given in Eq. (13). The average and variance of photons absorbed (emitted) within a finite time interval t can be determined as,

$$\begin{aligned} \langle N_{a(e)} \rangle = & -\partial_{s_{a(e)}}\theta(s_a, s_e)|_{s_a, s_e=0}t \\ = & \frac{\gamma_w x_{a(e)}(2\gamma_m + \gamma_w x_{e(a)})}{4\gamma_m + 2\langle n \rangle\gamma_w + \gamma_w}t, \end{aligned} \quad (15)$$

and,

$$\begin{aligned} \langle \Delta N_{a(e)}^2 \rangle = & \partial_{s_{a(e)}}^2\theta(s_a, s_e)|_{s_a, s_e=0}t \\ = & \langle N_{a(e)} \rangle - \frac{2\gamma_w^2 x_{a(e)}^2 (2\gamma_m + \gamma_w x_{e(a)})^2 t}{(4\gamma_m + 2\langle n \rangle\gamma_w + \gamma_w)^3}. \end{aligned} \quad (16)$$

where $x_a = \langle n \rangle$ and $x_e = \langle n \rangle + 1$. Given the expression of variance, it is evident that it is consistently less than the mean, indicating a sub-Poissonian photon distribution for both the absorption and emission events separately. Simultaneous monitoring of both the radiative events gives more compelling statistics as will be discussed in detail in Sec. III B. The average number of total jumps in this case is,

$$\langle \tilde{N}_o \rangle = \langle N_e \rangle + \langle N_a \rangle, \quad (17)$$

which can be thought of as the statistical observable for the negation of null events (hence the subscript “o”). The variance of the sum of absorption and emission events can be computed as,

$$\langle \Delta \tilde{N}_o^2 \rangle = \langle \Delta N_e^2 \rangle + \langle \Delta N_a^2 \rangle + 2\text{Cov}(N_e, N_a), \quad (18)$$

where $\text{Cov}(N_e, N_a) = \partial_{s_a s_e}^2 \theta(s_a, s_e)|_{s_a, s_e=0}t$ is the covariance of the observed absorption and emission events, given by,

$$\begin{aligned} \text{Cov}(N_e, N_a) = & \frac{\gamma_w^2 x_a x_e \{8\gamma_m^2 + 4\gamma_m(2\gamma_w\langle n \rangle + \gamma_w) + \gamma_w^2 [2x_a x_e + 1]\}}{(4\gamma_m + 2\gamma_w\langle n \rangle + \gamma_w)^3}t. \end{aligned} \quad (19)$$

We use the Mandel’s Q parameter, defined as [6, 7],

$$Q = \frac{\langle \Delta N^2 \rangle - \langle N \rangle}{\langle N \rangle}, \quad (20)$$

to quantify the quantumness of observed events. Mandel’s Q ranges between $-1 < Q < 0$ for sub-Poissonian statistics, $Q = 0$ for Poissonian statistics, and $Q > 0$ for super-Poissonian statistics. For the absorption (or emission) event, we obtain the following Mandel’s Q,

$$\begin{aligned} Q_{a(e)} = & -\frac{\partial_{s_{a(e)}}^2\theta(s_a, s_e)|_{s_a, s_e=0}}{\partial_{s_{a(e)}}\theta(s_a, s_e)|_{s_a, s_e=0}} - 1 \\ = & -\frac{2\gamma_w x_{a(e)}(2\gamma_m + \gamma_w x_{e(a)})}{(4\gamma_m + 2\langle n \rangle\gamma_w + \gamma_w)^2}, \end{aligned} \quad (21)$$

As discussed, with the rapid refreshing of the detector, the observable statistics are sub-Poissonian for both the absorption and emission events. The Mandel’s Q parameter \tilde{Q}_o can be calculated similarly for the sum of absorption and emission events (the negation of null events). We obtain,

$$\begin{aligned} \tilde{Q}_o = & \frac{-4\gamma_m^2\gamma_w + x_a x_e \gamma_w^3}{(\gamma_m(2\langle n \rangle + 1) + x_a x_e \gamma_w)(4\gamma_m + (2\langle n \rangle + 1)\gamma_w)^2}. \end{aligned} \quad (22)$$

A. The precision of quantum jump events

The statistics of absorption or emission events, when monitored individually, are sub-Poissonian ($-1 < Q < 0$) as shown in Fig. 2. When $\langle n \rangle \neq 0$, the statistics of absorption and emission events are maximally sub-Poissonian in the absence of continuous quantum measurements of the spin ($\gamma_m = 0$) yielding,

$$Q_{a(e)}^{\min.} = -\frac{2\langle n \rangle(\langle n \rangle + 1)}{(2\langle n \rangle + 1)^2} \rightarrow -4/9 \text{ in the limit } \langle n \rangle \rightarrow 1. \quad (23)$$

We also note that the asymptotic value of $Q_{a(e)}^{\min.} \rightarrow -1/2$ in the limit $\langle n \rangle \rightarrow \infty$. A good measure of the regularity of the quantum jumps, apart from Mandel's Q parameter, is the relative error, $\Delta N/\langle N \rangle$ (where ΔN is the standard deviation). Such a measure is applicable, for instance, if one were to keep track of the number of quantum jumps to measure the time elapsed as in a radio-carbon clock [42]. If observing either the absorption or the emission events is used as a clock signal, our findings suggest that such a quantum clock would achieve the following optimal relative error,

$$\lim_{\langle n \rangle \rightarrow \infty} \frac{\Delta N_{a(e)}}{\langle N_{a(e)} \rangle} = \lim_{\langle n \rangle \rightarrow \infty} \frac{\sqrt{1+Q}}{\sqrt{\langle N_{a(e)} \rangle}} \rightarrow \frac{1}{\sqrt{2\langle N_{a(e)} \rangle}}. \quad (24)$$

Note that, in comparison to a radio-carbon clock which is Poissonian ($Q = 0$), using either the absorption or emission as the time-reference can improve the clock's precision [defined as $\langle N_{a(e)} \rangle^2 / \Delta N_{a(e)}^2$] by a factor of two. Practically, note that even the limit $\langle n \rangle \rightarrow 1$ offers an improvement in precision by a factor of $9/5 = 1.8$, close to the asymptotic ($\langle n \rangle \rightarrow \infty$) result.

B. A spin-measurement induced transition in the observable statistics

Keeping track of both the absorption and emission events equally introduces an interesting variability in the observable statistics. From Eq. (22), we note that the corresponding statistics can be sub-Poissonian, Poissonian, or super-Poissonian, depending on the continuous spin measurement rate. In the absence of continuous spin measurements ($\gamma_m \rightarrow 0$),

$$\tilde{Q}_o \rightarrow (2\langle n \rangle + 1)^{-2} > 0, \quad (25)$$

suggesting that the observable statistics will be super-Poissonian, approaching Poissonian in the limit of large n . The observable statistics, however also change, as we increase the rate at which the quantum emitter's Pauli spin is continuously monitored along the transition dipole. While we see super-Poissonian statistics ($Q > 0$) for low values of γ_m , the statistics continuously transition into sub-Poissonian statistics by increasing γ_m (see

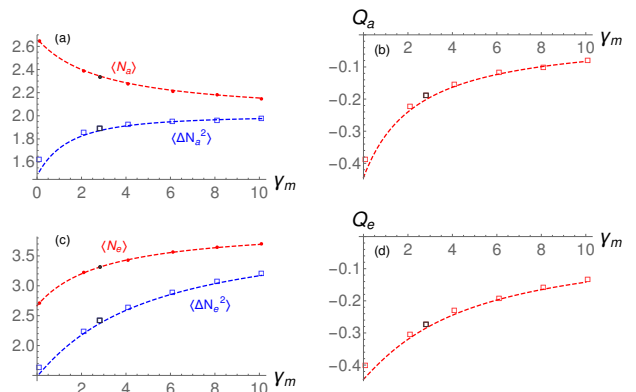


FIG. 2. Characterizing the statistics of absorption and emission events: (a) and (c) show the mean and variance of the photons absorbed and emitted respectively. We use $\Omega = 1$, $\gamma_w = 4$ and $\langle n \rangle = 1$. In the simulations, the moments are calculated over 8×10^4 trajectories, using 2000 time steps with a time increment of $dt = 5 \times 10^{-4}$. Each trajectory is initialized in the steady state ρ_s of the unconditional dynamics. (b) and (d) shows Mandel's Q parameters for absorption and emission events respectively. The dashed lines are predictions based on the large deviation principle.

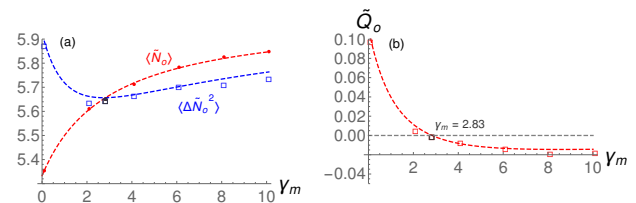


FIG. 3. Characterizing the statistics of the sum of absorption and emission events, using the same parameters as in Fig. 2: (a) Mean and variance of the sum of absorption and emission events. (b) The Mandel's Q parameter, with transition point ($Q=0$) at $\gamma_m = 2.83$. The statistics corresponding to the transition point are shown in black. The dashed lines are predictions based on the large deviation principle.

Fig. 3 and Fig. 4.). The value of γ_m at which the transition happens is

$$2\gamma_m = \gamma_w \sqrt{\langle n \rangle^2 + \langle n \rangle}, \quad (26)$$

where the statistics are Poissonian. Rewriting Eq. (12) in the traditional Lindblad form, we can think of $2\gamma_m$ as the rate corresponding to the Lindblad dissipator $L = \sigma_x$, and we see that the transition point we obtain is the geometric mean of the other two transition rates, $\gamma_w \langle n \rangle$ (corresponding to $L = \hat{\sigma}_+$) and $\gamma_w (\langle n \rangle + 1)$ (corresponding to $L = \hat{\sigma}_-$).

IV. CONCLUSIONS

We characterized the statistics of the radiative processes of a measurement-driven quantum emitter us-

ing the large deviation principle. The quantum emitter was driven by continuously monitoring the Pauli spin $\hat{\sigma}_x$ along its transition dipole, a direction of spin that maximally non-commutes with the Hamiltonian of the quantum emitter. We find that the statistics of observed quantum jumps is generically sub-Poissonian. Given it is known that coherently driven atoms can produce sub-Poissonian statistics [6, 7], the interest here lies in the observation that a seemingly incoherent process (measurement-induced dephasing), as opposed to coherent driving, generates the non-classical photon statistics [29]. The quantumness here can be attributed to the maximal non-commutativity of the observed Pauli spin $\hat{\sigma}_x$ along the transition dipole to the Hamiltonian of the quantum emitter. We also observe that the statistics of the negation of null detection events where the detector did not make a quantum jump can be very informative of the underlying dynamics, as this statistical observable undergoes a quantum measurement-driven transition from super-Poissonian to sub-Poissonian statistics as a function of the Pauli spin measurement rate. In the limit where the photodetector is initially in the vacuum state, our results naturally reproduce the statistics of resonant fluorescence, which is sub-Poissonian [6, 7, 29, 45].

There have been important recent developments in clever ways to address nuclear transitions, which also shed light on the difficulty in exciting desired atomic or nuclear transitions in general [38, 39]. Inducing transitions using engineering quantum measurement interactions can be very relevant in these contexts too, where it may have the potential to stimulate transitions that are difficult to achieve in practice by using traditional alternatives such as applying coherent drives.

The quantum emission scenarios we consider can also be very useful for artificial atom-based quantum technologies in practice. Initially populated photodetectors present a realistic scenario in photodetection, and their finite-time statistics are naturally significant in a variety of disciplines ranging from quantum thermodynamics to quantum sensing. It also applies to the paradigm of flying qubits and free-space quantum optics for optimal atom-photon interactions [46, 47]. Our work also suggests a number of future directions worth exploring further, that leverage the unique properties of the statistics of the sum of absorption and emission events, which also gives useful insights on the instances where the quantum

emitter did not make a jump. Our results are generalizable to the case of driven atoms, and to driven atoms which are continuously monitored. They encompass various avenues of contemporary interest in quantum thermodynamics [29, 35, 41–43, 48–53].

We conclude by noting some limitations to our present approach. Firstly, our results only make use of a leading order estimate for the large deviation form of the exact moment-generating function, which can be potentially improved further [54, 55]. We also limit our considerations to the linear order in perturbation theory that is generically valid for small $\gamma_w \langle n \rangle dt \ll 1$, corresponding to the exchange of zero or one photon with the optical environment. Owing to the rotating wave approximation we make, combined with the rapid refreshing of the environment, we do not see any signatures of different quantum states of the optical environment, other than its average occupation. While the linearized and perturbative regime within the rotating wave approximation encompasses a range of scenarios we are currently interested in, we note that potential generalizations are very interesting [30, 31]. We also see that our predictions start to deviate, especially in the negated null statistics, for higher occupations of the field, $\langle n \rangle > 1$. Here higher-order corrections become non-negligible suggesting that our treatment needs to be generalized further. We defer such considerations to future work.

V. ACKNOWLEDGMENTS

SKM thanks Andrew Jordan, Supriya Krishnamurthy, Pranay Nayak, and Sreeram PG for discussions on related topics and Andrea Maiani and Igor Pikovski for helpful suggestions. The work of SKM is supported in part by the Swedish Research Council under Contract No. 335-2014-7424 and in part by the Wallenberg Initiative on Networks and Quantum Information (WINQ). This collaboration was made possible through the Nordita Summer Internship Program in Theoretical Physics, 2024. We extend our sincere thanks to Ivan Khymovich for his valuable support.

Data availability statement—The numerical simulations (using Mathematica [56]) associated with the article can be accessed in the following [Github repository link](#).

Appendix A: Measurement operators for observable radiative processes

We consider the quantum emitter initialized in an arbitrary, pure initial state, $|\Psi_s\rangle = \alpha|e\rangle + \beta|g\rangle$. To derive the measurement operators corresponding to the absorption, emission, and the null events, we first consider a simple scenario where the quantum emitter is coupled to an excited state of the optical field, $|n\rangle$. The state of the combined system in time dt is,

$$|\Psi_{dt}\rangle = e^{-i\hat{H}_{int}dt}|\Psi_s\rangle|n\rangle, \quad (\text{A1})$$

where the interaction Hamiltonian we consider satisfies $\hat{H}_{int}dt = \sqrt{\gamma_w dt}(\hat{\sigma}_+\hat{a} + \hat{\sigma}_-\hat{a}^\dagger)$ [28]. Here γ_w is the spontaneous emission rate of the quantum emitter, $\hat{\sigma}_+$ and $\hat{\sigma}_-$ are the raising and lowering operators of the emitter, and \hat{a}^\dagger and \hat{a} are the creation and annihilation operators for the optical field.

Taylor expanding the time-evolution operator $e^{-i\sqrt{\gamma_w dt}(\hat{\sigma}_+\hat{a} + \hat{\sigma}_-\hat{a}^\dagger)}$ till linear order in dt , we obtain,

$$|\Psi_{dt}\rangle \approx \left[\hat{1} - i\sqrt{\gamma_w dt}(\hat{\sigma}_+\hat{a} + \hat{\sigma}_-\hat{a}^\dagger) - \frac{\gamma_w dt}{2} (|e\rangle\langle e|(\hat{a}^\dagger\hat{a} + 1) + |g\rangle\langle g|\hat{a}^\dagger\hat{a}) \right] |\Psi_s\rangle|n\rangle. \quad (\text{A2})$$

The measurement operator corresponding to no photon detection (null event) is obtained by projecting to $|n\rangle$,

$$\begin{aligned} \hat{M}_w(o) &= \langle n|\Psi_{dt}\rangle \\ &= \begin{pmatrix} 1 - \frac{\gamma_w dt(n+1)}{2} & 0 \\ 0 & 1 - \frac{\gamma_w dt n}{2} \end{pmatrix} \\ &\approx \begin{pmatrix} \sqrt{1 - (n+1)\gamma_w dt} & 0 \\ 0 & \sqrt{1 - n\gamma_w dt} \end{pmatrix}. \end{aligned} \quad (\text{A3})$$

Similarly, the measurement operators corresponding to emission and absorption are,

$$\hat{M}_w(e) = \langle n+1|\Psi_{dt}\rangle = -i \begin{pmatrix} 0 & 0 \\ \sqrt{(n+1)\gamma_w dt} & 0 \end{pmatrix}, \quad (\text{A4})$$

$$\hat{M}_w(a) = \langle n-1|\Psi_{dt}\rangle = -i \begin{pmatrix} 0 & \sqrt{n\gamma_w dt} \\ 0 & 0 \end{pmatrix}. \quad (\text{A5})$$

The above results assumes that the optical field, or the photodetector is always reset to a Fock state. We will now consider potential generalizations to the above measurement operators. For an arbitrary initial state of the field, $|\psi_F\rangle$, we can write $|\Psi_{dt}\rangle$ in matrix form as,

$$|\Psi_{dt}\rangle \approx \begin{pmatrix} 1 - \gamma_w dt(\hat{a}^\dagger\hat{a} + 1)/2 & -i\hat{a}\sqrt{\gamma_w dt} \\ -i\hat{a}^\dagger\sqrt{\gamma_w dt} & 1 - \gamma_w dt(\hat{a}^\dagger\hat{a})/2 \end{pmatrix} |\Psi_s\rangle|\psi_F\rangle. \quad (\text{A6})$$

Similarly, for a generic density matrix $\rho_s \otimes \rho_F$, we may write,

$$\begin{aligned} \rho_{dt} &\approx \begin{pmatrix} 1 - \gamma_w dt(\hat{a}^\dagger\hat{a} + 1)/2 & -i\hat{a}\sqrt{\gamma_w dt} \\ -i\hat{a}^\dagger\sqrt{\gamma_w dt} & 1 - \gamma_w dt(\hat{a}^\dagger\hat{a})/2 \end{pmatrix} \rho_s \otimes \rho_F \begin{pmatrix} 1 - \gamma_w dt(\hat{a}^\dagger\hat{a} + 1)/2 & i\hat{a}\sqrt{\gamma_w dt} \\ i\hat{a}^\dagger\sqrt{\gamma_w dt} & 1 - \gamma_w dt(\hat{a}^\dagger\hat{a})/2 \end{pmatrix} \\ &= \hat{\mathcal{M}}_a \rho_s \otimes \rho_F \hat{\mathcal{M}}_a^\dagger + \hat{\mathcal{M}}_e \rho_s \otimes \rho_F \hat{\mathcal{M}}_e^\dagger + \hat{\mathcal{M}}_o \rho_s \otimes \rho_F \hat{\mathcal{M}}_o^\dagger, \end{aligned} \quad (\text{A7})$$

where we have identified,

$$\hat{\mathcal{M}}_e = \begin{pmatrix} 0 & 0 \\ -i\hat{a}^\dagger\sqrt{\gamma_w dt} & 0 \end{pmatrix}, \quad \hat{\mathcal{M}}_a = \begin{pmatrix} 0 & -i\hat{a}\sqrt{\gamma_w dt} \\ 0 & 0 \end{pmatrix}, \quad (\text{A8})$$

and,

$$\hat{\mathcal{M}}_o = \begin{pmatrix} 1 - \gamma_w dt(\hat{a}^\dagger\hat{a} + 1)/2 & 0 \\ 0 & 1 - \gamma_w dt(\hat{a}^\dagger\hat{a})/2 \end{pmatrix}. \quad (\text{A9})$$

These operators satisfy the completeness relation,

$$\sum_{i \in \{a, e, o\}} \text{tr}_F[\rho_F \hat{\mathcal{E}}_i] = \sum_{i \in \{a, e, o\}} \hat{E}_i \approx \hat{1}_{2 \times 2}, \quad (\text{A10})$$

where $\hat{\mathcal{E}}_i = \hat{\mathcal{M}}_i^\dagger \hat{\mathcal{M}}_i$, and the effect operators (or POVM elements) defined as $\hat{E}_i = \text{tr}_F[\rho_F \hat{\mathcal{E}}_i]$. We find that,

$$\hat{E}_e = \begin{pmatrix} \text{tr}\{\rho_F(\hat{a}\hat{a}^\dagger)\}\gamma_w dt & 0 \\ 0 & 0 \end{pmatrix} = \begin{pmatrix} (\langle n \rangle + 1)\gamma_w dt & 0 \\ 0 & 0 \end{pmatrix}, \quad (\text{A11})$$

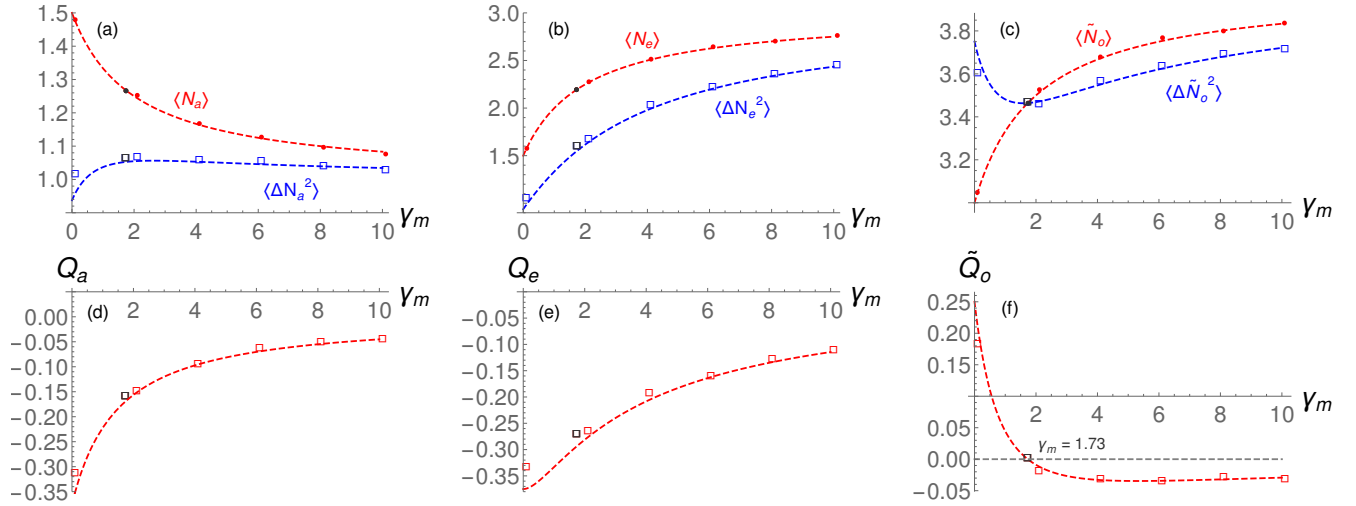


FIG. 4. Statistics of the radiative processes in an optical environment with average occupation number $\langle n \rangle = 0.5$: Panels (a) and (b) shows the mean and variance of photons absorbed and emitted respectively and the panels (d) and (e) are the corresponding Mandel's Q parameters. The dashed lines are predictions of the large deviation principle. We assume parameters otherwise identical to Figs.2 and 3. Figs.(c) and (f) shows the statistics of the negation of null events (sum of absorption and emission events), with the transition from super-Poissonian to sub-Poissonian statistics occurring at $\gamma_m = 1.73$. The transition point from simulations is also shown in black.

$$\hat{E}_a = \begin{pmatrix} 0 & 0 \\ 0 & \text{tr}\{\rho_F(\hat{a}^\dagger \hat{a})\} \gamma_w dt \end{pmatrix} = \begin{pmatrix} 0 & 0 \\ 0 & \langle n \rangle \gamma_w dt \end{pmatrix}, \quad (\text{A12})$$

and

$$\hat{E}_o = \begin{pmatrix} 1 - \text{tr}\{\rho_F(\hat{a} \hat{a}^\dagger)\} \gamma_w dt & 0 \\ 0 & 1 - \text{tr}\{\rho_F(\hat{a}^\dagger \hat{a})\} \gamma_w dt \end{pmatrix} = \begin{pmatrix} 1 - (\langle n \rangle + 1) \gamma_w dt & 0 \\ 0 & 1 - \langle n \rangle \gamma_w dt \end{pmatrix}. \quad (\text{A13})$$

We have denoted $\text{tr}\{\rho_F \hat{a}^\dagger \hat{a}\} = \langle n \rangle$, the average occupation of the optical environment. We now resolve the effect operators (or POVM elements) to the following measurement operators which are similar in form to the once we found before. However, now they are better understood as the coarse-grained measurement operators that correspond to absorption, emission, or null events in the quantum emitter in arbitrary optical environments,

$$\hat{M}_e = -i \begin{pmatrix} 0 & 0 \\ \sqrt{(\langle n \rangle + 1) \gamma_w dt} & 0 \end{pmatrix}, \quad \hat{M}_a = -i \begin{pmatrix} 0 & \sqrt{\langle n \rangle \gamma_w dt} \\ 0 & 0 \end{pmatrix}, \quad (\text{A14})$$

and,

$$\hat{M}_o = \begin{pmatrix} \sqrt{1 - (\langle n \rangle + 1) \gamma_w dt} & 0 \\ 0 & \sqrt{1 - \langle n \rangle \gamma_w dt} \end{pmatrix}. \quad (\text{A15})$$

Here we have only imposed $\hat{M}_i^\dagger \hat{M}_i = \hat{E}_i$ for $i \in \{a, e, o\}$. Generically, the average occupation $\langle n \rangle$ can be a continuous variable, as opposed to the case when the detector is in a number state. It can be verified that the unconditional evolution generated by these measurement operators to leading order reproduces the Gorini-Kossakowski-Sudarshan-Lindblad form of the master equation given in the main text. Note that we have limited ourselves to the rotating wave approximated interaction Hamiltonian from the beginning, and therefore interesting quantum effects, such as the effect of a squeezed reservoir if present [30, 31], does not appear in the dynamics to linear order. However our present approach to determine the statistics can be potentially generalized beyond the rotating wave approximation as well. We defer these considerations to future work.

- [1] L. Novotny and B. Hecht, Quantum emitters, in *Principles of Nano-Optics* (Cambridge University Press, 2012) pp. 282–312.
- [2] L. Mandel and E. Wolf, *Optical Coherence and Quantum Optics* (Cambridge University Press, 1995).
- [3] M. Fortsch, J. U. Furst, C. Wittmann, D. Strekalov, A. Aiello, M. V. Chekhova, C. Silberhorn, G. Leuchs, and C. Marquardt, A versatile source of single photons for quantum information processing, *Nature Communications* **4**, 1818 (2013), publisher: Nature Publishing Group.
- [4] J. Yang, M. Khanahmadi, I. Strandberg, A. Gaikwad, C. Castillo-Moreno, A. F. Kockum, M. A. Ullah, G. Johansson, A. M. Eriksson, and S. Gasparinetti, *Deterministic generation of frequency-bin-encoded microwave photons* (2024), arXiv:2410.23202.
- [5] C. Castillo-Moreno, K. R. Amin, I. Strandberg, M. Kervinen, A. Osman, and S. Gasparinetti, *Dynamical excitation control and multimode emission of an atom-photon bound state* (2024), arXiv:2404.05547.
- [6] L. Mandel, Sub-Poissonian photon statistics in resonance fluorescence, *Optics Letters* **4**, 205 (1979), publisher: Optica Publishing Group.
- [7] R. Short and L. Mandel, Observation of Sub-Poissonian Photon Statistics, *Physical Review Letters* **51**, 384 (1983), publisher: American Physical Society.
- [8] L. Davidovich, Sub-poissonian processes in quantum optics, *Rev. Mod. Phys.* **68**, 127 (1996).
- [9] A. N. Jordan and I. A. Siddiqi, *Quantum Measurement: Theory and Practice* (Cambridge University Press, 2024) google-Books-ID: MRrxEAAAQBAJ.
- [10] A. N. Korotkov and A. N. Jordan, Undoing a weak quantum measurement of a solid-state qubit, *Phys. Rev. Lett.* **97**, 166805 (2006).
- [11] A. N. Jordan and A. N. Korotkov, Uncollapsing the wavefunction by undoing quantum measurements, *Contemporary Physics* **51**, 125 (2010), publisher: Taylor & Francis .eprint: <https://doi.org/10.1080/00107510903385292>.
- [12] S. K. Manikandan and F. Wilczek, *Detecting Acoherence in Radiation Fields* (2024), arXiv:2409.20378.
- [13] E. M. Purcell, Spontaneous emission probabilities at radio frequencies, in *Confined Electrons and Photons* (Springer, 1995) pp. 839–839.
- [14] G. S. Agarwal, Quantum statistical theories of spontaneous emission and their relation to other approaches, in *Quantum Optics*, edited by G. Hohler (Springer Berlin Heidelberg, Berlin, Heidelberg, 1974) pp. 1–128.
- [15] P. Lewalle, S. K. Manikandan, C. Elouard, and A. N. Jordan, Measuring fluorescence to track a quantum emitter’s state: a theory review, *Contemporary Physics* **61**, 26 (2020), publisher: Taylor & Francis .eprint: <https://doi.org/10.1080/00107514.2020.1747201>.
- [16] A. N. Jordan, A. Chantasri, P. Rouchon, and B. Huard, Anatomy of fluorescence: quantum trajectory statistics from continuously measuring spontaneous emission, *Quantum Studies: Mathematics and Foundations* **3**, 237 (2016).
- [17] Z. K. Mineev, S. O. Mundhada, S. Shankar, P. Reinhold, R. Gutierrez-Jauregui, R. J. Schoelkopf, M. Mirrahimi, H. J. Carmichael, and M. H. Devoret, To catch and reverse a quantum jump mid-flight, *Nature* **570**, 200 (2019), publisher: Nature Publishing Group.
- [18] S. K. Manikandan, C. Elouard, and A. N. Jordan, Fluctuation theorems for continuous quantum measurements and absolute irreversibility, *Phys. Rev. A* **99**, 022117 (2019).
- [19] B. Kannan, M. J. Ruckriegel, D. L. Campbell, A. Frisk Kockum, J. Braumüller, D. K. Kim, M. Kjaergaard, P. Krantz, A. Melville, B. M. Niedzielski, A. Vepsäläinen, R. Winik, J. L. Yoder, F. Nori, T. P. Orlando, S. Gustavsson, and W. D. Oliver, Waveguide quantum electrodynamics with superconducting artificial giant atoms, *Nature* **583**, 775 (2020), publisher: Nature Publishing Group.
- [20] H. M. Wiseman and Z. Brady, Robust unravelings for resonance fluorescence, *Phys. Rev. A* **62**, 023805 (2000).
- [21] P. Campagne-Ibarcq, P. Six, L. Bretheau, A. Sarlette, M. Mirrahimi, P. Rouchon, and B. Huard, Observing quantum state diffusion by heterodyne detection of fluorescence, *Phys. Rev. X* **6**, 011002 (2016).
- [22] Q. Ficheux, S. Jezouin, Z. Leghtas, and B. Huard, Dynamics of a qubit while simultaneously monitoring its relaxation and dephasing, *Nature Communications* **9**, 1926 (2018), publisher: Nature Publishing Group.
- [23] C. Joshi, F. Yang, and M. Mirhosseini, Resonance fluorescence of a chiral artificial atom, *Phys. Rev. X* **13**, 021039 (2023).
- [24] H. Hutin, A. Essig, R. Assouly, P. Rouchon, A. Bienfait, and B. Huard, Monitoring the energy of a cavity by observing the emission of a repeatedly excited qubit, *Phys. Rev. Lett.* **133**, 153602 (2024).
- [25] P. Campagne-Ibarcq, S. Jezouin, N. Cottet, P. Six, L. Bretheau, F. Mallet, A. Sarlette, P. Rouchon, and B. Huard, Using spontaneous emission of a qubit as a resource for feedback control, *Phys. Rev. Lett.* **117**, 060502 (2016).
- [26] A. Essig, Q. Ficheux, T. Peronin, N. Cottet, R. Lescanne, A. Sarlette, P. Rouchon, Z. Leghtas, and B. Huard, Multiplexed photon number measurement, *Phys. Rev. X* **11**, 031045 (2021).
- [27] Note that traditional photodetectors are reset rapidly typically to their quantum ground state. This also ensures they are in the Markovian regime of operation with no memory effects.
- [28] J. A. Gross, C. M. Caves, G. J. Milburn, and J. Combes, Qubit models of weak continuous measurements: markovian conditional and open-system dynamics, *Quantum Science and Technology* **3**, 024005 (2018), publisher: IOP Publishing.
- [29] S. K. Manikandan, Autonomous quantum clocks using athermal resources, *Phys. Rev. Res.* **5**, 043013 (2023).
- [30] H. J. Carmichael, A. S. Lane, and D. F. Walls, Resonance fluorescence from an atom in a squeezed vacuum, *Phys. Rev. Lett.* **58**, 2539 (1987).
- [31] D. M. Toyli, A. W. Eddins, S. Boutin, S. Puri, D. Hover, V. Bolkhovskiy, W. D. Oliver, A. Blais, and I. Siddiqi, Resonance fluorescence from an artificial atom in squeezed vacuum, *Phys. Rev. X* **6**, 031004 (2016).
- [32] S. Pilgram, A. N. Jordan, E. V. Sukhorukov, and M. Büttiker, Stochastic path integral formulation of full counting statistics, *Phys. Rev. Lett.* **90**, 206801 (2003).
- [33] E. V. Sukhorukov, A. N. Jordan, S. Gustavsson,

- R. Leturcq, T. Ihn, and K. Ensslin, Conditional statistics of electron transport in interacting nanoscale conductors, *Nature Physics* **3**, 243 (2007), publisher: Nature Publishing Group.
- [34] D. A. Bagrets and Y. V. Nazarov, Full counting statistics of charge transfer in coulomb blockade systems, *Phys. Rev. B* **67**, 085316 (2003).
- [35] G. T. Landi, M. J. Kewming, M. T. Mitchison, and P. P. Potts, Current fluctuations in open quantum systems: Bridging the gap between quantum continuous measurements and full counting statistics, *PRX Quantum* **5**, 020201 (2024).
- [36] C. L. Degen, F. Reinhard, and P. Cappellaro, Quantum sensing, *Rev. Mod. Phys.* **89**, 035002 (2017).
- [37] A. D. Ludlow, M. M. Boyd, J. Ye, E. Peik, and P. O. Schmidt, Optical atomic clocks, *Rev. Mod. Phys.* **87**, 637 (2015).
- [38] C. Zhang, T. Ooi, J. S. Higgins, J. F. Doyle, L. von der Wense, K. Beeks, A. Leitner, G. A. Kazakov, P. Li, P. G. Thirolf, T. Schumm, and J. Ye, Frequency ratio of the 229mTh nuclear isomeric transition and the 87Sr atomic clock, *Nature* **633**, 63 (2024), publisher: Nature Publishing Group.
- [39] J. Tiedau, M. V. Okhapkin, K. Zhang, J. Thielking, G. Zitzer, E. Peik, F. Schaden, T. Pronebner, I. Morawetz, L. T. De Col, F. Schneider, A. Leitner, M. Pressler, G. A. Kazakov, K. Beeks, T. Sikorsky, and T. Schumm, Laser excitation of the th-229 nucleus, *Phys. Rev. Lett.* **132**, 182501 (2024).
- [40] A. D. Panov, Quantum Zeno Effect, Nuclear Conversion and Photoionization in Solids, *Annals of Physics* **249**, 1 (1996).
- [41] X. He, P. Pakkiam, A. A. Gangat, M. J. Kewming, G. J. Milburn, and A. Fedorov, Effect of measurement back-action on quantum clock precision studied with a superconducting circuit, *Phys. Rev. Appl.* **20**, 034038 (2023).
- [42] G. J. Milburn, The thermodynamics of clocks, *Contemporary Physics* **61**, 69 (2020), publisher: Taylor & Francis eprint: <https://doi.org/10.1080/00107514.2020.1837471>.
- [43] P. Erker, M. T. Mitchison, R. Silva, M. P. Woods, N. Brunner, and M. Huber, Autonomous quantum clocks: Does thermodynamics limit our ability to measure time?, *Phys. Rev. X* **7**, 031022 (2017).
- [44] K. Jacobs and D. A. Steck, A straightforward introduction to continuous quantum measurement, *Contemporary Physics* **47**, 279 (2006), publisher: Taylor & Francis eprint: <https://doi.org/10.1080/00107510601101934>.
- [45] J. P. Garrahan and I. Lesanovsky, Thermodynamics of Quantum Jump Trajectories, *Physical Review Letters* **104**, 160601 (2010), publisher: American Physical Society.
- [46] N. Trautmann, G. Alber, and G. Leuchs, Efficient single-photon absorption by a trapped moving atom, *Phys. Rev. A* **94**, 033832 (2016).
- [47] M. Stobinska, G. Alber, and G. Leuchs, Perfect excitation of a matter qubit by a single photon in free space, *Europhysics Letters* **86**, 14007 (2009).
- [48] L. M. Cangemi, C. Bhadra, and A. Levy, *Quantum Engines and Refrigerators* (2023), arXiv:2302.00726 [quant-ph].
- [49] C. Elouard, D. A. Herrera-Martín, M. Clusel, and A. Aufferes, The role of quantum measurement in stochastic thermodynamics, *npj Quantum Information* **3**, 1 (2017), publisher: Nature Publishing Group.
- [50] M. Ferri-Cortes, J. A. Almanza-Marrero, R. Lopez, R. Zambrini, and G. Manzano, *Entropy production and fluctuation theorems for monitored quantum systems under imperfect detection* (2024), arXiv:2308.08491.
- [51] G. Manzano, J. M. Horowitz, and J. M. R. Parrondo, Quantum fluctuation theorems for arbitrary environments: Adiabatic and nonadiabatic entropy production, *Phys. Rev. X* **8**, 031037 (2018).
- [52] S. Sundelin, M. A. Aamir, V. M. Kulkarni, C. Castillo-Moreno, and S. Gasparinetti, *Quantum refrigeration powered by noise in a superconducting circuit* (2024), arXiv:2403.03373.
- [53] J. A. M. Guzman, P. Erker, S. Gasparinetti, M. Huber, and N. Y. Halpern, *Useful autonomous quantum machines* (2024), arXiv:2307.08739.
- [54] F. Carollo, R. L. Jack, and J. P. Garrahan, Unraveling the large deviation statistics of markovian open quantum systems, *Phys. Rev. Lett.* **122**, 130605 (2019).
- [55] F. Carollo, J. P. Garrahan, and R. L. Jack, Large Deviations at Level 2.5 for Markovian Open Quantum Systems: Quantum Jumps and Quantum State Diffusion, *Journal of Statistical Physics* **184**, 13 (2021).
- [56] W. R. Inc., Mathematica, Version 12.0, champaign, IL, 2019.